Earth Reinforcement, Ochiai, Yasufuku & Omine (eds) © 1996 Balkema, Rotterdam. ISBN 90 5410 833 9

Localized deformation analysis of reinforced foundation ground

K.Yamamoto & J.Otani
Kumamoto University, Japan

ABSTRACT: This paper describes not only the bearing capacity but also the failure mechanism of reinforced foundation ground using rigid plastic finite element method. Here, the analysis includes the effect of geometry change for the purpose of evaluating the failure mechanism, quantitatively. In order to take into account the reinforcing effect in the analysis, a composite type of model including reinforcing material and the surrounding soil is proposed. The effectiveness of the proposed method is verified by comparing with the results of model loading test.

1 INTRODUCTION

Analysis methods for bearing capacity of reinforced foundation ground so far mainly depend on limit equilibrium method which must assume location and shape of the failure surface. In the current design method, it is assumed that the failure mechanism of reinforced ground is same as that of non-reinforced ground such as the mechanism proposed by Terzaghi(1943). And the real failure mechanism of the reinforced foundation ground has not been investigated and in fact, this is more progressive type of failure than that of the non-reinforced ground because of the tensile property of the reinforcing materials. Meanwhile, in recent years, a rigid plastic finite element technique which is different type of limit analysis using finite element formulation has been used for geotechnical engineering problems(for example,Tamura et al.1984 and Kodaka et al.1995). One of the distinguished point for this technique is unnecessity of the assumption on the location and shape of the failure surface.

The purpose of this paper is to analyze bearing capacity and failure mechanism of reinforced foundation ground using rigid plastic finite element method. The effectiveness of the analysis method proposed in this study is evaluated by comparing the results of model loading test in which the ground was modeled by aluminum rods. In order to investigate the effect of localized deformation in the ground, the analysis is also conducted with the effect of geometry change and the validity of this effect is evaluated.

2 TEST RESULTS

The paper by Otani et al.(1996) has described the details of the model loading tests. The precise contents of this loading test are omitted in this paper.

The relation between the loading pressure and the settlement of the loading plate for all cases are shown in Fig.1 where B is the width of loading plate, and b and z are the length and the depth of reinforcing materials, respectively. This paper describes the analysis results of reinforced foundation ground by paper as the reinforcing material in the comparative study.

3 METHOD OF ANALYSIS AND REINFORCED SOIL MODEL

3.1 *Method of analysis*

Tamura et al.(1984) have formulated a rigid-plastic finite element method (RPFEM) to the stability analysis in geotechnical engineering field and this method is used for calculating bearing capacity of reinforced foundation ground. The formulation of RPFEM is summarized briefly on the basis of the references by Tamura et al.(1984) and Otani et al.(1994).

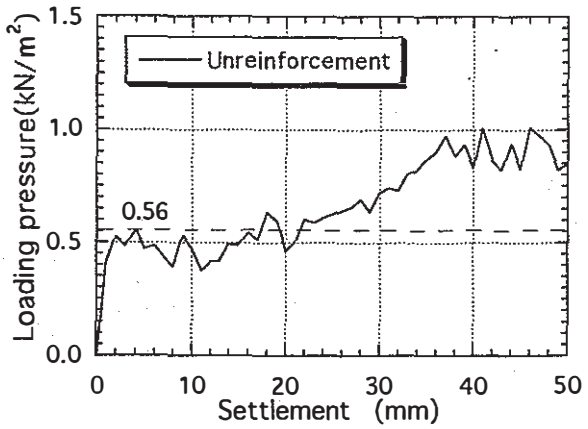

(a) unreinforced ground

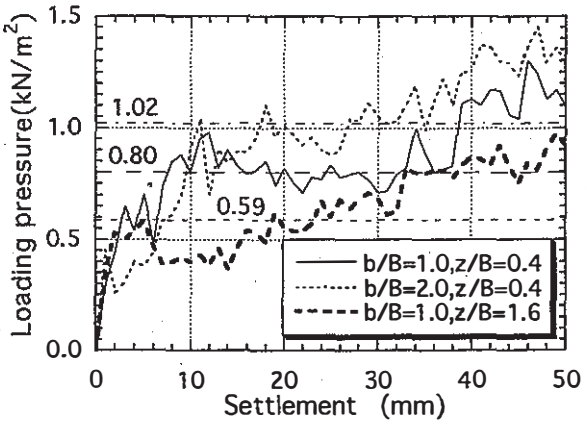

(b) reinforced foundation ground

Fig.1 Loading pressure-settlement curve.

The displacement control type of RPFEM which prescribe displacement velocities at the displacement boundary corresponding to the model loading test condition was used as a analysis method and is resulted a contact pressure distribution of the foundation ground at the limit state. Note that rigid rough footing was assumed in this study. For the constitutive equations, Drucker-Prager models are used for the ground by aluminum rods (c-ϕ materials) and that is

$$f = -\alpha I_1 + \sqrt{J_2} = k \qquad (1)$$

where I_1 is the first invariant of stress σ_{ij}, J_2 is the second invariant of deviatoric stress s_{ij}. α and k are the material constants, respectively. The formulation of this RPFEM is employed in the following form by introducing the Lagrange multipliers λ, μ.

$$\int_V B^T s dV + L^T \lambda = C^T \mu \qquad (2)$$

$$L\dot{u} + \frac{3\alpha}{\left(3\alpha^2 + 1/2\right)^{1/2}} \dot{\bar{e}} = 0 \qquad (3)$$

$$C\dot{u} = \dot{u}_0 \qquad (4)$$

where B : matrix defined such as $\dot{\varepsilon} = B\dot{u}$
L : matrix defined such as $\dot{v} = L\dot{u}$
C : matrix for substitute one at necessary location
s : vector of deviatoric stresses s_{ij}
$\dot{u}$: vector of nodal velocities
$\dot{u}_0$: vector of nodal velocities defined from displacement velocities boundary conditions
$\dot{v}$: vector of rates of volumetric change
$\dot{\bar{e}}$: equivalent plastic strain rate ($\dot{\bar{e}} = \sqrt{\dot{\varepsilon}_{ij}\dot{\varepsilon}_{ij}}$)
α : parameter for isotropic stress dependency of shear strength
λ : indeterminate isotropic stress vector (Lagrange multiplier)
μ : nodal force vector indicated as a contact pressure distribution (Lagrange multiplier)

Eq.2 indicates the equilibrium equation of forces at limit state and accompanies two constraint conditions (Eq.3 and Eq.4). The first constraint condition, Eq.3 indicates volumetric strain condition at all elements in the limit state. The vector $\dot{u}_0$ is a prescribed vector only at the displacement velocity boundary and the matrix C retrieves the displacement velocity vector at the displacement velocity boundary when all the nodal vector of the displacement velocities, $\dot{u}$ are multiplied by C. Therefore, the second constraint condition, Eq.4 defines the provisional norms of velocity vector beneath the rigid loading plate. In RPFEM, the constitutive equation is governed by only associated flow rule and then,

$$\dot{\varepsilon}_{ij} = \Lambda \frac{\partial f}{\partial \sigma_{ij}} \qquad (5)$$

in which Λ is an indeterminate multiplier.
Substituting Eq.5 into Eq.2, Eq.2 is solved iteratively by replacing $\dot{u}$ to $\dot{u} + \beta\Delta\dot{u}$ using Newton-Raphson method because Eq.2 has nonlinear characteristic where β is a converge parameter. Note that $\beta = 0.2$ for unreinforced case and $\beta = 0.01 \sim 0.05$ for reinforced one are used here in this study. Finally, the both Lagrange multipliers λ and μ, and the displacement velocities field $\dot{u}$ are obtained at the

limit state. The bearing capacity of this RPFEM is evaluated as an average value of a contact pressure integrated by the foundation footing and the resultant displacement velocity field may be considered to be a plastic flow in the failure zone. In addition, the rigid-plastic finite element analysis with and without the effect of geometry change are conducted to investigate the influence of the localized deformation in this study. The analysis method with the effect of geometry change assumes the velocity field to be a displacement increment per unit time, and step-by-step calculation due to incremental applied displacement on the loading plate is carried out by renewing the coordinate system as a result of deformation.

3.2 *Reinforced soil model*

There are two basic ideas of modeling the interaction behavior between soil and reinforcing material. One is that the soil and reinforcing material are individually modeled, and the other is that the reinforcing material and the surrounding soil are unified in the model. When the former is used to solve nonlinear differential equation, the large difference of the stiffness between soil and reinforcing material is very crucial for the conversion of the solution by Newton-Raphson method. The sand layer is usually constructed around the reinforcing material in the clayey ground for the purpose of increasing the friction between the reinforcing material and the ground. Here in the paper, the latter is used as the model of the reinforced soil shown in Fig.2, in which the reinforcing material and the surrounding sand layers are assumed to be a unique material as a composite material. The equivalent cohesion, C_{uR} for this composite material is evaluated by following equation:

$$C_{uR} = \frac{T\sqrt{K_P}}{2\Delta H} \tag{6}$$

where T and K_P are tensile strength of the reinforcing material and passive earth pressure coefficient of sand, respectively. ΔH is the range of reinforcing effect. This equation was originally developed by Schlosser et al.(1973) based on the laboratory test results. The assumption on this equation is that the average strain at the direction of the reinforcing material in sand is always equal to the elongation of the reinforcing material, so that the stress increment due to the reinforcing effect is obtained from the tensile strength of the reinforcing material at the limit state with the confining pressure by passive earth pressure. It is noted that the relative displacement between reinforcing material and sand is neglected in this model.

4 RESULTS AND DISCUSSION

The finite element mesh used in this analysis is shown in Fig.3. First of all, the soil parameters such as cohesion, c and the angle of internal friction, ϕ are determined by back analysis using the model test result of bearing capacity of unreinforced ground q_0=0.56kN/m^2(cf. Fig.1(a)). These are c=2.5KN/m^2 and ϕ = 25°. The resultant plastic flow of the unreinforced ground are shown in Fig.4 with the soil parameters. The case of reinforced foundation ground by paper(tensile strength T= 2.4 kN/m) is also analyzed using these parameters with proposed reinforced soil model and the results for the cases changing the length and the depth of reinforcing material(paper) are shown in Fig.5. As clearly shown from these results, the area of existing plastic flow for the reinforced case in Fig.5(a),(b) is extended widely towards the bottom of the model ground comparing that for the unreinforced

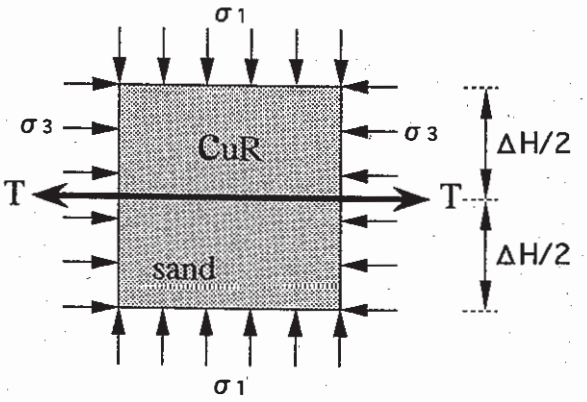

Fig.2 Reinforced soil model in plane strain condition.

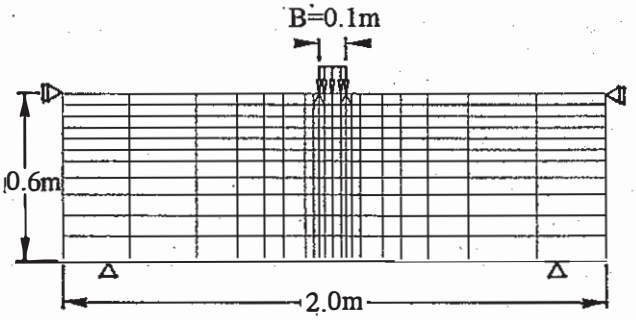

Fig.3 Finite element mesh.

case(Fig.4), and the resultant bearing capacities increase. Comparing Figs.5(a) and (b) on the purpose of the effect of the length, the area of plastic flow is a little wider only laterally but its bearing capacity is totally improved as the length of the reinfircement increases. The result in Fig.5(c) is the case for the placement of the reinforcement deeper than other cases which are indicated in Figs.5(a) and (b). The failure mechanism of this case is very similar to that of unreinforced case in Fig.4. Thus, it may be said that there should be an optimum depth of the reinforcement for the purpose of expecting the maximum improved bearing capacity, and this was also observed on the model loading tests as shown in Fig.1(b).

The analysis results obtained so far are based on the concept of upper bound theorem on rigid-plastic theory, so that the effect of geometrical nonlinearity which plays a important roll on the localized deformation analysis is not taken into account. As expressed in 3.1, this analysis with the effect of geometry changes was also conducted by assuming the velocity field to be a displacement increment per unit time. Then, the step-by-step calculation for applied displacement on the loading plate was carried out. It is noted that here in the analysis, the results at the settlement level, S/B=0.4 is depicted. Fig.6 shows a result of unreinforced case while the reinforced cases are shown in Fig.7. The cases analyzed here are the same as those in Figs.4 and 5. Again, it is concluded from these figures that the earth reinforcement makes the failure zone wide but not the vertical direction. The improved bearing capacities obtained for the reinforced cases are also fairly close to those of test results.

Photo 1 to Photo 4 are shown the test results of model ground by aluminum rods for not only the unreinforced case but also the reinforced cases which are the same cases as the analysis. The behavior of these pictures are very similar to those of the analysis results shown in Figs.6 and 7. Thus, the consideration of geometry change in rigid-plastic finite element analysis is necessary and the effectiveness of proposed analysis method is also verified.

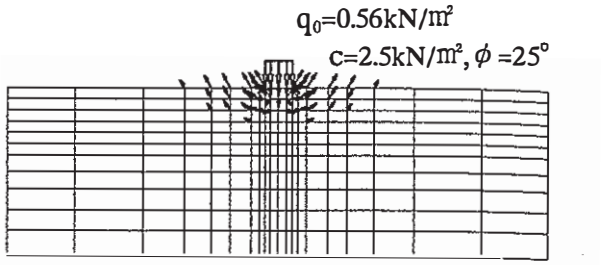

Fig.4 Resultant soil parameters and plastic flow for unreinforced ground.

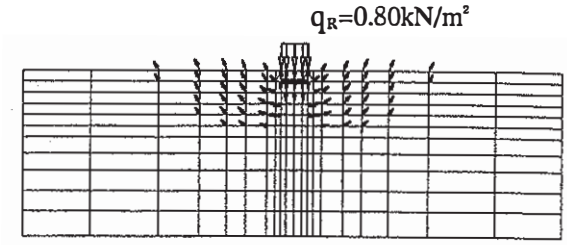

(a) b/B=1.0,z/B=0.4

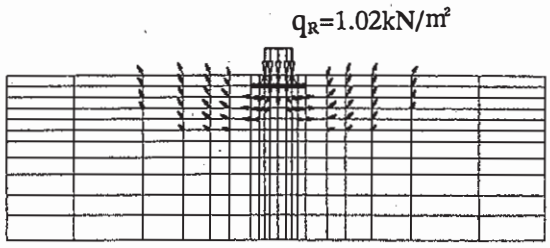

(b) b/B=2.0,z/B=0.4

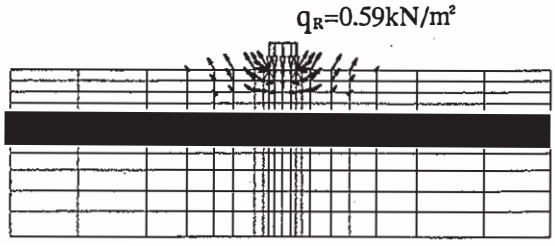

(c) b/B=1.0,z/B=1.6

Fig.5 Bearing capacity and plastic flow for reinforced foundation ground.

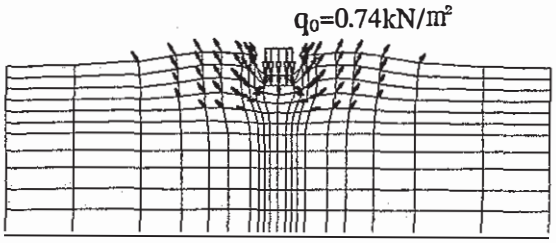

Fig.6 Bearing capacity and plastic flow considering geometry change for unreinforced ground (S/B=0.4).

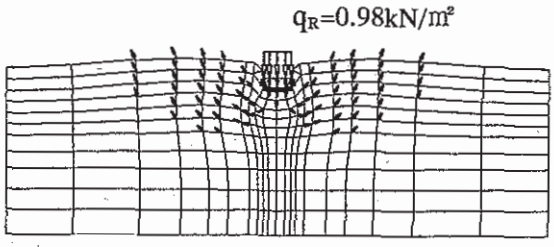

(a) b/B=1.0,z/B=0.4

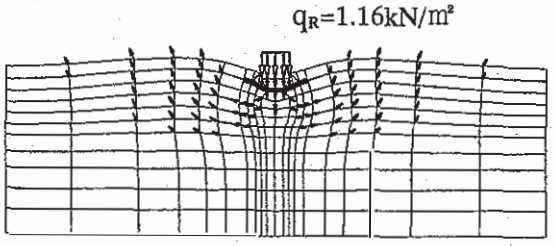

(b) b/B=2.0,z/B=0.4

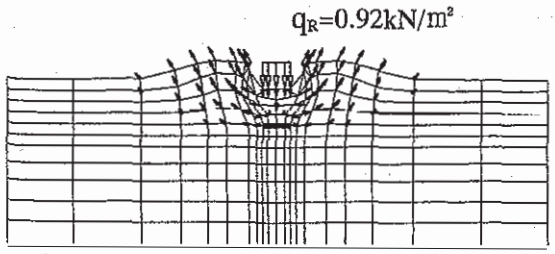

(c) b/B=1.0,z/B=1.6

Fig.7 Bearing capacity and plastic flow considering geometry change for reinforced foundation ground (S/B=0. 4).

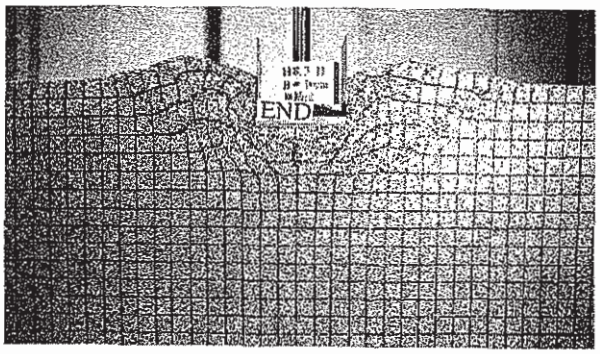

Photo 1. Failure mechanism of unreinforced ground (S/B=0. 5).

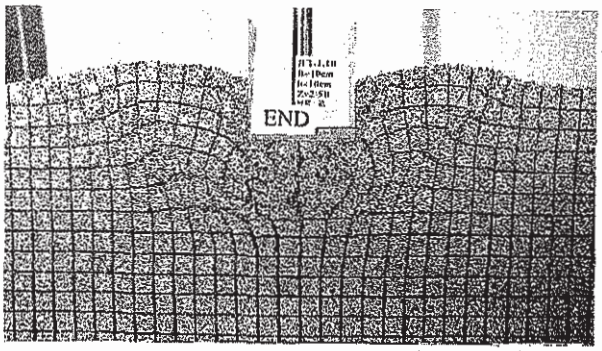

Photo 2. Failure mechanism of reinforced foundation ground (reinforcing material: paper,b/B=1.0,z/B=0.4, S/B=0. 5).

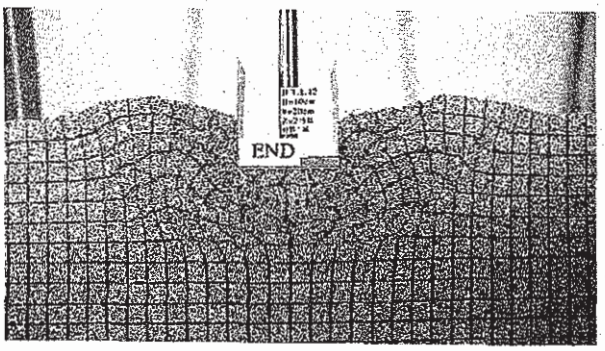

Photo 3. Failure mechanism of reinforced foundation ground (reinforcing material: paper,b/B=2.0,z/B=0.4, S/B=0. 5).

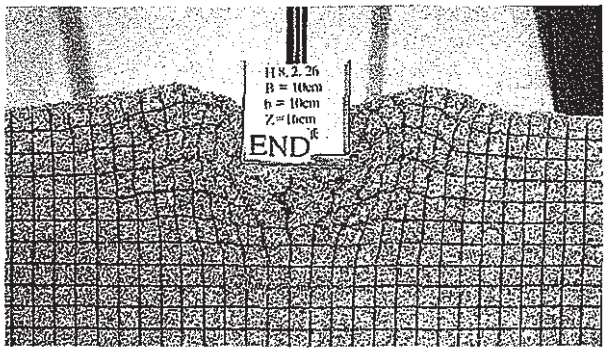

Photo 4. Failure mechanism of reinforced foundation ground (reinforcing material: paper,b/B=1.0,z/B=1.6, S/B=0. 5).

5 CONCLUSIONS

Not only the bearing capacity but also the failure mechanism of the reinforced foundation ground were analyzed using rigid finite element method with and without the effect of geometrical nonlinearity. Here, in order to model the reinforced soil in the analysis, the model of unifying the reinforcing material with its surrounding soil proposed by the authors was used. Based on the analysis results in this study, it is concluded that the rigid-plastic finite element technique is very useful method for even earth reinforcement structures when the proposed reinforced model is used, and after including the effect of geometrical nonlinearity in this method, the both improved bearing capacity and the failure mechanism are evaluated more quantitatively with acceptable accuracy.

ACKNOWLEGEMENT

The authors would like to express their gratitude to Professor Tamura of Kyoto University, Japan for his sincere advice on this study.

REFERENCES

Kodaka, T., Asaoka, A. and Pokharel, G. 1995. Model tests and theoretical analysis of reinforced soil slopes with facing panels. Soils and Foundations, Vol.35, No.1, pp.133-145.

Levy, N., Marcal,P.V., Ostergren, W.J. and Rice,J.R. 1971. Small scale yielding near a crack in plane strain: a finite element analysis. International Journal of Fracture Mechanics, Vol.7, No.2, pp.143-156.

Otani, J., Ochiai, H., Miyata, Y. 1994. Bearing capacity of geogrid reinforced grounds. Fifth Int. Conference on Geotextiles, Geomembranes and Related Products, Singapore, Vol.1, pp.117-120.

Otani, J., Yamamoto, K. 1996. Experimental study on localized deformation behavior of reinforced foundation ground. Proc. of Int. Symposium on Earth Reinforcement, Fukuoka, (to appear).

Schlosser, F. and Long, N.T. 1973. Etude dn comportement du Materiaux Terre Armée. Annales de L' Institut Technique de Batiment et des Travaux Pablic, Supplement No. 304, Series Matériaux No. 45.

Tamura, T., Kobayashi, S. and Sumi, T. 1987. Rigid-plastic finite element method for frictional materials. Soils and Foundations, Vol.27, No.3, pp.1-12.

Terzaghi, K. 1943. Theoretical Soil Mechanics. John Wiley Sons.